

Title

A new murine model of Barth Syndrome neutropenia links TFAZZIN deficiency to increased ER stress induced apoptosis

Authors

Jihee Sohn, Jelena Milosevic, Thomas Brouse, Najihah Aziz, Jenna Elkhoury, Suya Wang, Alexander Hauschild, Nick van Gastel, Murat Cetinbas, Sara F. Tufa, Douglas R. Keene, Ruslan I. Sadreyev, William T. Pu, David B. Sykes

Supplemental Figure Legends

Figure S1. Validation of WT- and TFAZZIN-KO genotypes by polymerase chain reaction (PCR) genotyping. (A) Two WT and two TFAZZIN-KO clones are displayed to highlight the published genotyping strategy. A 2% agarose gel was used to resolve the PCR products. (B) An example of the expected results from the gender genotyping PCR are displayed to highlight how to distinguish female and male embryos.

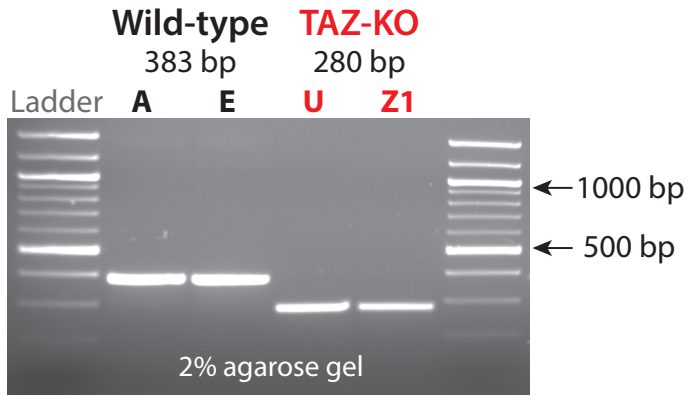
Figure S2. Analysis of adult hematopoiesis in the setting of TFAZZIN deficiency: Trial #2. (A) The frequency of CD45.2 donor cells, both WT and TFAZZIN-KO, in the peripheral blood remains stable following transplantation out to 16-weeks. (B) Complete blood counts of the peripheral blood demonstrate a mild leukopenia in mice transplanted with TFAZZIN-KO fetal liver cells. Hematocrit and platelet counts are not altered in the setting of TFAZZIN deficiency. (C) Flow cytometry was used to enumerate specific populations within the peripheral blood, with a focus on the transplanted CD45.2 cells. The lack of TFAZZIN results in significantly fewer B-cells, T-cells, myeloid cells, and neutrophils. (D) Flow cytometry gating strategy for identifying mature cells in the peripheral blood. (E) Flow cytometry gating strategy for identifying myeloid progenitors in the bone marrow. Error bars indicate the mean \pm SD. T-tests were performed. $**P < .01$; $***P < .001$; $****P < .0001$. NS=not statistically significant.

Figure S3. The lack of TFAZZIN does not affect morphology, mitochondrial content, or transwell migration. (A) Wright-Giemsa staining and 100x oil light micrographs of WT and TFAZZIN-KO GMP progenitors [(+)E2] and mature neutrophils [(-)E2 4-days]. (B) Mitochondria were quantified by comparing copies of mitochondrial DNA to genomic DNA by quantitative RT-PCR. This experiment was performed three times and the data was combined and is displayed. (C) Analysis of mitochondrial mass using Mitotracker staining and quantification by flow cytometry was performed in both GMPs and mature neutrophils and normalized to the wild-type clones. (D) Neutrophil migration towards LPS (100 ng/ml) was assayed by transwell migration. (E) Wright-Giemsa staining and 100x oil light micrographs of WT and TFAZZIN-KO primary adult bone marrow neutrophils. Error bars indicate the mean \pm SD. T-tests were performed. NS=not statistically significant.

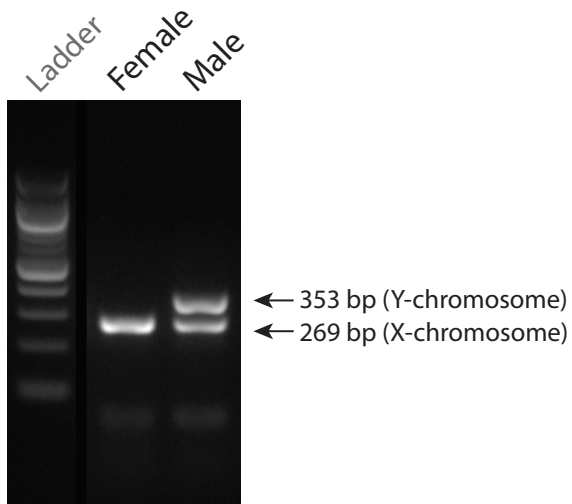
Figure S4. The lack of TFAZZIN results in ultrastructural changes in mitochondria. (A) WT and TFAZZIN-KO progenitors. Mitochondria cristae tended to be more distinct in the WT (black arrows, upper right), with spiral structures more prevalent in the KO (white arrow, lower right). Although not specific to the KO, mitochondria tended to be encircled by rough endoplasmic reticulum (RER, black arrows, lower right). The density of the mitochondria lumen was greater in the WT. Scale bars: left panels 2 μ m; right panels 500 nm. (B) WT and TFAZZIN-KO mature neutrophils. The size of the mitochondria was approximately equal, with well-defined cristae more commonly resolved in the WT neutrophils (black arrows, upper right). Spiral structures with the lumen of the mitochondria were occasionally noted in WT but were considerably more prevalent in the KO neutrophils (black arrows, lower right). Autophagosomes were present in both groups but were considerably more prevalent in the KO (white arrows, lower right). Scale bars: left panels 2 μ m; right panels 500 nm. (C) TFAZZIN-KO progenitors. Mitochondria were commonly encircled by RER (black arrows). Spiral structures within the lumen of the mitochondria were common (white arrows). Scale bar = 500 nm.

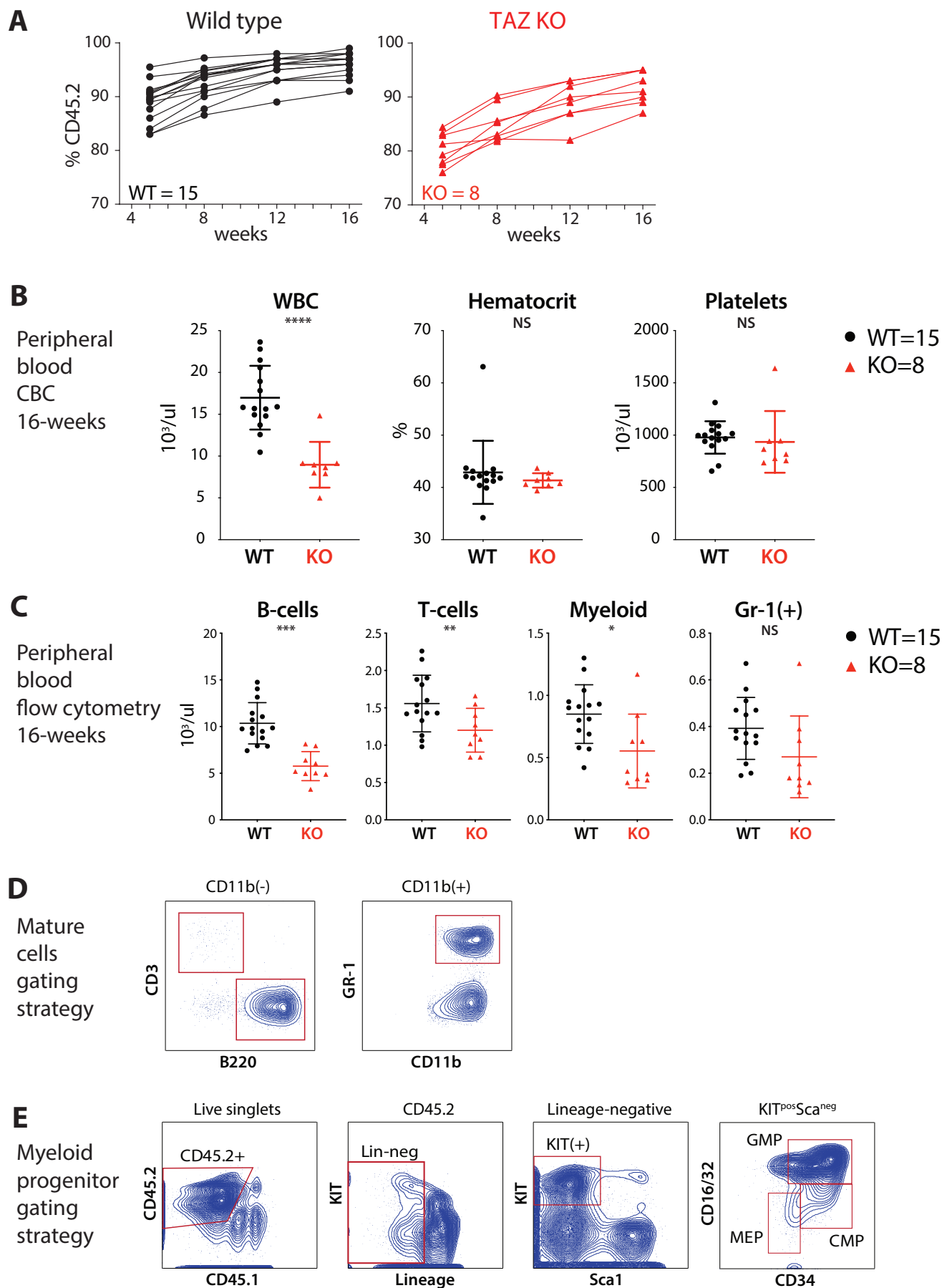
Figure S5. TFAZZIN deficient myeloid progenitors are more sensitive to apoptosis and ER stress signals. (A) ER-Hoxb8 GMP were set up in 96-well plate format and viability was assessed *in vitro* (CellTiter Glo®) at 24-hours after exposure to ABT199, AMG176, or Thapsigargin. This assay was performed on >5 different days with multiple clones; the total N is displayed on each graph. This same data without error bars is displayed in Figure 7A. A two-way analysis of variance (ANOVA) was used to determine the statistical difference between viability curves. (B) Primary fetal liver hematopoietic cells from the embryos derived from three timed pregnancy litters were set up in 96-well plate format and viability was assessed *in vitro* (CellTiter Glo®) at 24-hours after exposure to ABT199. (C) Flow cytometry gating strategy for identification of the CD45.2 lymphoid and myeloid cells within the peripheral blood.

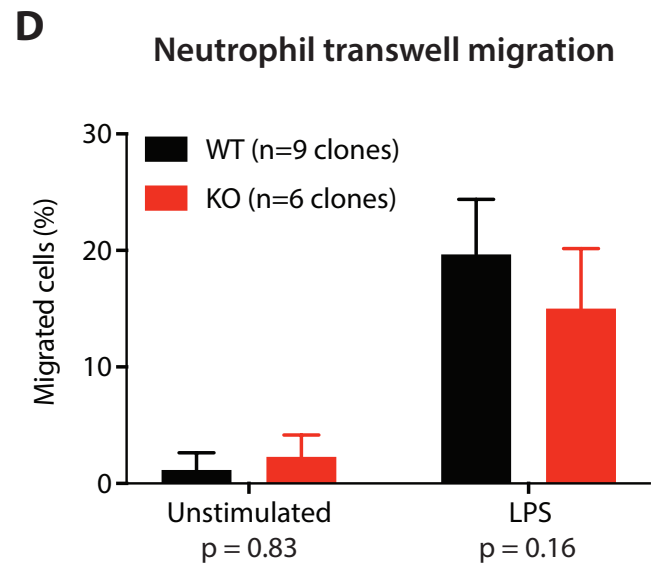
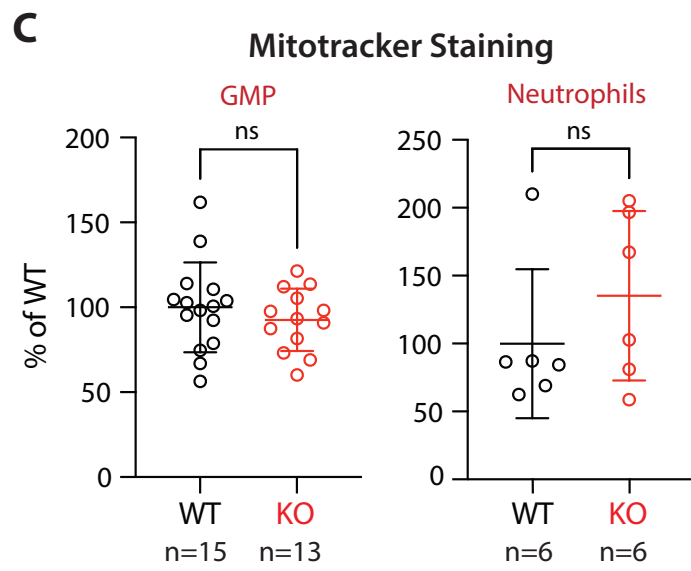
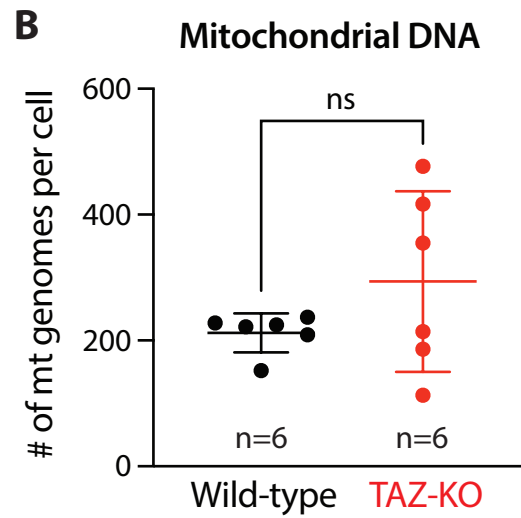
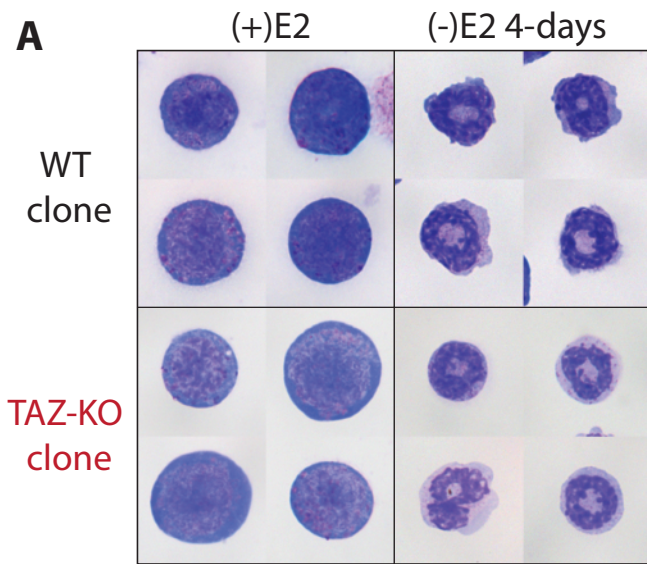
A TFAZZIN Genotyping PCR



B Gender Genotyping PCR







E Primary bone marrow adult neutrophils

